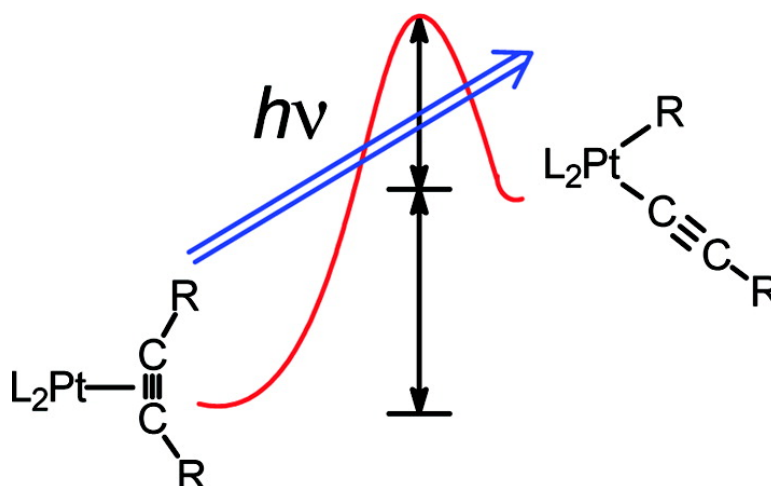


Cleavage of Carbon–Carbon Bonds of Diphenylacetylene and Its Derivatives via Photolysis of Pt Complexes: Tuning the C–C Bond Formation Energy toward Selective C–C Bond Activation

Ahmet Gunay, and William D. Jones

J. Am. Chem. Soc., **2007**, 129 (28), 8729-8735 • DOI: 10.1021/ja071698k • Publication Date (Web): 20 June 2007

Downloaded from <http://pubs.acs.org> on February 16, 2009



More About This Article

Additional resources and features associated with this article are available within the HTML version:

- Supporting Information
- Links to the 2 articles that cite this article, as of the time of this article download
- Access to high resolution figures
- Links to articles and content related to this article
- Copyright permission to reproduce figures and/or text from this article

[View the Full Text HTML](#)



ACS Publications
 High quality. High impact.

Cleavage of Carbon–Carbon Bonds of Diphenylacetylene and Its Derivatives via Photolysis of Pt Complexes: Tuning the C–C Bond Formation Energy toward Selective C–C Bond Activation

Ahmet Gunay and William D. Jones*

Contribution from the Department of Chemistry, University of Rochester,
Rochester, New York 14627

Received March 10, 2007; E-mail: jones@chem.rochester.edu

Abstract: Carbon–carbon bond activation of diphenylacetylene and several substituted derivatives has been achieved via photolysis and studied. Pt⁰–acetylene complexes with η^2 -coordination of the alkyne, along with the corresponding Pt^{II} C–C activated photolysis products, have been synthesized and characterized, including X-ray crystal structural analysis. While the C–C cleavage reaction occurs readily under photochemical conditions, thermal activation of the C–C bonds or formation of Pt^{II} complexes was not observed. However, the reverse reaction, C–C reductive coupling (Pt^{II} \rightarrow Pt⁰), did occur under thermal conditions, allowing the determination of the energy barriers for C–C bond formation from the different Pt^{II} complexes. For the reaction (dtbpe)Pt(–Ph)(–C \equiv CPh) (**2**) \rightarrow (dtbpe)Pt(η^2 -PhC \equiv CPh) (**1**), ΔG^\ddagger was 32.03–(3) kcal/mol. In comparison, the energy barrier for the C–C bond formation in an electron-deficient system, that is, (dtbpe)Pt(C₆F₅)(C \equiv CC₆F₅) (**6**) \rightarrow (dtbpe)Pt(η^2 -bis(pentafluorophenyl)acetylene) (**5**), was found to be 47.30 kcal/mol. The energy barrier for C–C bond formation was able to be tuned by electronically modifying the substrate with electron-withdrawing or electron-donating groups. Upon cleavage of the C–C bond in (dtbpe)Pt(η^2 -(*p*-fluorophenyl)-*p*-tolylacetylene) (**9**), both (dtbpe)Pt(*p*-fluorophenyl)(*p*-tolylacetylidene) (**10**) and (dtbpe)Pt(*p*-tolyl)(*p*-fluorophenylacetylidene) (**11**) were obtained. Kinetic studies of the reverse reaction confirmed that **10** was more stable toward the reductive coupling [the term “reductive coupling” is defined as the formation of (dtbpe)Pt(η^2 -acetylene) complex from the Pt^{II} complex] than **11** by 1.22 kcal/mol, under the assumption that the transition-state energies are the same for the two pathways. The product ratio for **10** and **11** was 55:45, showing that the electron-deficient C–C bond is only slightly preferentially cleaved.

Introduction

Activation of C–C bonds with the help of the transition metal complexes remains one of the most challenging fields in organometallic chemistry.^{1–4} These fascinating reactions have attracted the attention of many chemists because of their potential applications in organic synthesis and petroleum and pharmaceutical research.⁵ While C–H bond activation has found many successful applications in organic synthesis and the chemical industry, C–C bond activation is far from practical use.⁵

Understanding the factors influencing C–C bond activation and figuring out the mechanism of metal insertion into the C–C bond will be key to the future development of this important field of organometallic chemistry.² In order to provide a driving force for C–C bond cleavage, relief of ring strain and attainment of aromaticity have been employed,^{6–13} as has forcing the target

C–C bond into close proximity to the transition metal center.^{1,2,14,15} A preliminary report from our group using bis(diisopropylphosphino)ethane, bis(di-*t*-butylphosphino)methane, and hemilabile diisopropylphosphinodimethylaminoethane chelates on platinum–acetylene complexes showed evidence for photochemical C–C cleavage.¹⁶ Here, this new method that does not take advantage of the aforementioned driving forces for C–C bond cleavage is further examined. A series of novel Pt⁰– η^2 -acetylene complexes has been synthesized and fully characterized along with their C–C bond-activated Pt^{II} counterparts.

- (1) Murakami, M.; Ito, Y. Cleavage of Carbon–Carbon Single Bonds by Transition Metals. In *Topics in Organometallic Chemistry*; Murai, S., Ed.; Springer: Berlin, 1999; Vol. 3, pp. 97–129.
- (2) Rybtchinski, B.; Milstein, D. *Angew. Chem., Int. Ed.* **1999**, *38*, 870–883.
- (3) Jennings, P. W.; Johnson, L. L. *Chem. Rev.* **1994**, *94*, 2241–2290.
- (4) Bishop, K. C., III. *Chem. Rev.* **1976**, *76*, 461–486.
- (5) Jun, C. H.; Moon, C. W.; Lee, H.; Lee, D. Y. *J. Mol. Catal. A* **2002**, *189*, 145–156.

- (6) Perthuisot, C.; Jones, W. D. *J. Am. Chem. Soc.* **1994**, *116*, 3647–3648.
- (7) Perthuisot, C.; Edelbach, B. L.; Zubris, D. L.; Jones, W. D. *Organometallics* **1997**, *16*, 2016–2023.
- (8) Edelbach, B. L.; Lachicotte, R. J.; Jones, W. D. *J. Am. Chem. Soc.* **1998**, *120*, 2843–2853.
- (9) Wick, D. D.; Northcutt, T. O.; Lachicotte, R. J.; Jones, W. D. *Organometallics* **1998**, *17*, 4484–4492.
- (10) Bessmertnykh, A. G.; Blinov, K. A.; Grishin, Y. K.; Donskaya, N. A.; Beletskaya, I. P. *Tetrahedron Lett.* **1995**, *36*, 7901–7904.
- (11) Nishimura, T.; Ohe, K.; Uemura, S. *J. Am. Chem. Soc.* **1999**, *121*, 2645–2646.
- (12) Nishimura, T.; Uemura, S. *J. Am. Chem. Soc.* **1999**, *121*, 11010–11011.
- (13) Jones, W. D. *Nature* **1993**, *364*, 676–677.
- (14) Rosenthal, U.; Pellny, P. M.; Kirchbauer, F. G.; Burlakov, V. V. *Acc. Chem. Res.* **2000**, *33*, 119–129.
- (15) Garcia, J. J.; Jones, W. D. *Organometallics* **2000**, *19*, 5544–5545.
- (16) Muller, C.; Iverson, C. N.; Lachicotte, R. J.; Jones, W. D. *J. Am. Chem. Soc.* **2001**, *123*, 9718–9719.

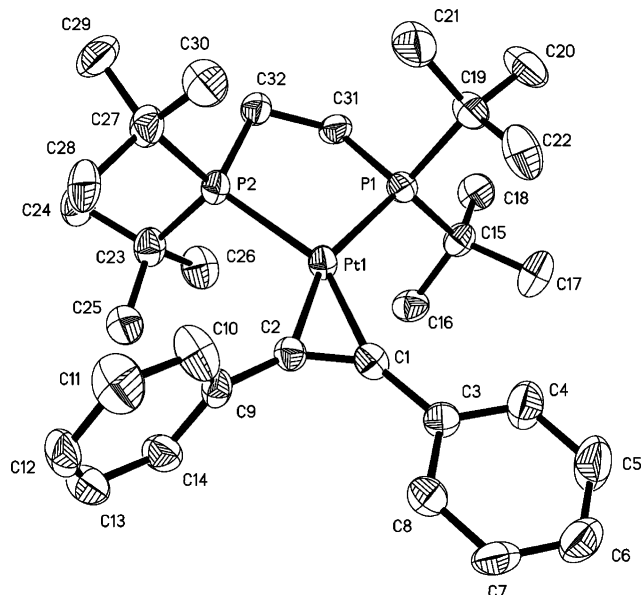


Figure 1. Molecular structure of (dtbpe)Pt(η^2 -PhC≡CPh) (**1**) (ORTEP, 30% probability ellipsoids).

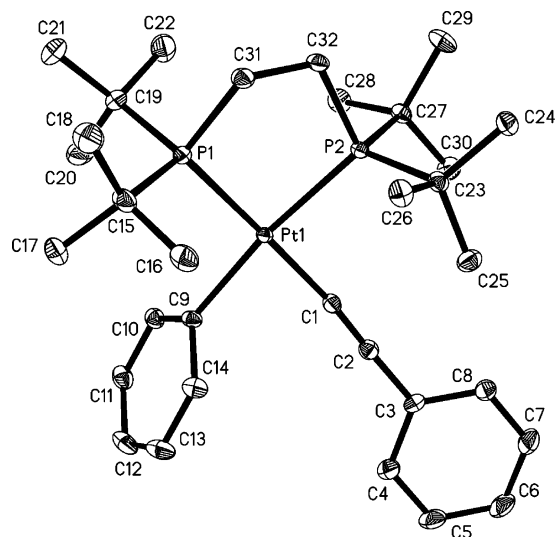


Figure 2. Molecular structure of (dtbpe)Pt^{II}(Ph)(phenylacetylide) (**2**) (ORTEP, 30% probability ellipsoids).

By modification of the aryl groups of the acetylene derivatives, the C–C bond formation energy could be tuned. A kinetic preference for C–C bond formation of the electron-rich Pt–aryl bond over the electron-poor Pt–aryl bond was investigated by using both electron-donating groups (EDG) and electron-withdrawing groups (EWG) as substituents on the aryl rings of the substrate.

Results and Discussion

In order to study C–C bond cleavage in aryl acetylenes, the η^2 -coordinated Pt⁰ complex (dtbpe)Pt(η^2 -PhC≡CPh) (**1**) was synthesized stoichiometrically by 1:1:1 ratio reaction of bis(*i*-*t*-butylphosphino)ethane (dtbpe), diphenylacetylene, and Pt(COD)₂ as shown in eq 1. Heating was required to produce only **1** as product. The ³¹P NMR spectrum of the product clearly showed the formation of **1** as a singlet at δ 94.23 with platinum satellites (¹*J*_{Pt–P} = 2516.4 Hz), which is typical for Pt⁰ complexes. The single-crystal structure of this Pt–acetylene

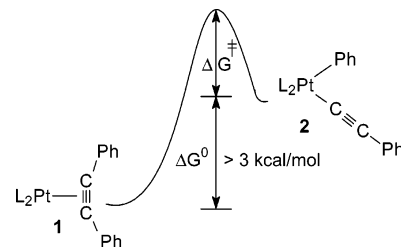
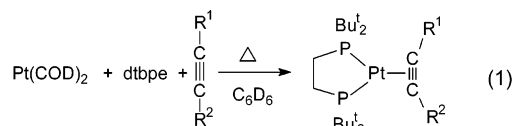


Figure 3. Energy profile of activation reaction.

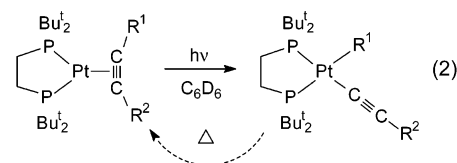
complex is depicted in Figure 1, and selected metrical data are given in Table 1.



1: R¹ = R² = phenyl; **3:** R¹ = R² = 3,5-xylyl; **5:** R¹ = R² = *p*-F-phenyl;
7: R¹ = R² = C₆F₅; **9:** R¹ = *p*-F-phenyl, R² = *p*-tolyl

While *d*¹⁰ Pt⁰ complexes might be expected to have a tetrahedral geometry, the structural analysis revealed a distorted square-planar geometry at the metal center with the alkyne ligand in the P–Pt–P plane. This distorted square-planar geometry can be explained in terms of π back-donation,^{17–19} which is suggested by an elongated C–C triple bond and bending of C≡C–C angles compared to free diphenylacetylene.²⁰ In addition, any π back-donation to the chelating phosphine (dtbpe) would also promote the formation of the observed geometry at the metal center.

To look for C–C bond activation, **1** was heated at 160 °C for 3 days. Under these conditions, no C–C bond cleavage or formation of Pt^{II} complex was observed. Under UV irradiation ($\lambda > 300$ nm), however, oxidative addition of the sp²–sp C–C bond was observed and (dtbpe)Pt(Ph)(phenylacetylide) (**2**) was produced in high yield (eq 2). Compound **1** has an absorption that tails into the near UV to ~ 360 nm (see Supporting Information). Product **2** displays two singlets in the ³¹P NMR spectrum at δ 71.36 and 77.45. Characteristic P–Pt coupling constants are seen for each phosphorus, with ¹*J*_{P–Pt} = 1978.3 Hz (trans to acetylide)²¹ and ¹*J*_{P–Pt} = 1250.6 Hz (trans to Ph).²² In addition, **2** was characterized by single-crystal X-ray diffraction as shown in Figure 2. The molecule has the expected square planar geometry for a Pt^{II} *d*⁸ complex, with the platinum-bound phenyl group lying at an angle of 80.9° to the square plane. Selected metrical data are given in Table 2.



2: R¹ = R² = phenyl; **4:** R¹ = R² = 3,5-xylyl;
6: R¹ = R² = *p*-F-phenyl; **8:** R¹ = R² = C₆F₅;
10: R¹ = *p*-F-phenyl, R² = *p*-tolyl; **11:** R¹ = *p*-tolyl, R² = *p*-F-phenyl

Upon heating the C–C activated complex **2**, reversion to the Pt⁰ complex **1** occurred. Therefore, even though the forward reaction does not proceed thermally, the reverse reductive coupling reaction does. Similar chemistry was observed earlier with the dippe analogue but was not quantified.¹⁶ These

Table 1. Selected Bond Lengths and Angles for **1**, **3**, **5**, **7**, and **9**

| | 1 | 3 | 5 | 7^a | 9 |
|-------------------|------------|------------|------------|----------------------|------------|
| Bond Lengths (Å) | | | | | |
| Pt(1)–P(1) | 2.2878(13) | 2.2951(9) | 2.2807(5) | 2.2676(8) | 2.2744(13) |
| Pt(1)–P(2) | 2.2823(14) | 2.2766(9) | 2.2860(5) | 2.2676(8) | 2.2913(13) |
| Pt(1)–C(1) | 2.056(5) | 2.055(3) | 2.0369(18) | 2.044(3) | 2.038(5) |
| Pt(1)–C(2) | 2.037(5) | 2.042(3) | 2.0553(18) | 2.044(3) | 2.044(5) |
| C(1)–C(2) | 1.299(6) | 1.303(5) | 1.309(2) | 1.295(6) | 1.304(7) |
| C(1)–C(3) | 1.455(6) | 1.456(5) | 1.458(3) | 1.456(4) | 1.454(7) |
| C(2)–C(9) | 1.466(6) | 1.460(5) | 1.465(2) | 1.456(4) | 1.463(7) |
| Bond Angles (deg) | | | | | |
| C(1)–Pt(1)–C(2) | 36.99(17) | 37.10(13) | 37.31(7) | 36.92(18) | 37.2(2) |
| C(2)–Pt(1)–P(2) | 113.32(14) | 114.50(10) | 121.50(5) | 117.19(9) | 121.02(16) |
| P(2)–Pt(1)–P(1) | 88.32(5) | 87.91(3) | 88.316(17) | 88.70(4) | 88.61(5) |
| P(1)–Pt(1)–C(1) | 121.43(14) | 120.09(10) | 112.92(5) | 117.19(9) | 112.36(15) |
| Pt(1)–P(1)–C(31) | 107.03(16) | 107.36(12) | 107.66(6) | 107.80(10) | 107.34(17) |
| Pt(1)–P(2)–C(32) | 108.41(16) | 108.38(12) | 107.39(6) | 107.80(10) | 107.33(17) |
| C(3)–C(1)–C(2) | 136.0(5) | 140.0(3) | 139.98(17) | 142.22(18) | 142.4(5) |
| C(9)–C(2)–C(1) | 143.9(5) | 142.5(3) | 135.55(17) | 142.22(18) | 138.8(5) |

^a Complex **7** sits on a crystallographic mirror plane bisecting the Pt₂ fragment. Therefore C1A, C2A, P1A, and C31A in complex **7** are listed here as C2, C9, P2, and C32, respectively.

observations indicate that the overall C–C cleavage process is *thermodynamically uphill* at [Pt(dtbpe)]. The free energy model shown in Figure 3 describes the situation best. The Pt^{II} complex must lie at a higher energy than the Pt⁰ complex because the reverse reaction proceeds spontaneously. Compound **1** does not observably convert to **2** thermally, indicating that **2** must be several kilocalories per mole higher in energy than **1**. To quantify the stability of the C–C cleavage product, **2** was heated at 80 °C and the reductive coupling reaction to form **1** was monitored by ³¹P NMR spectroscopy. The first-order rate constant (*k*) for the reverse reaction was determined by the slope of a plot of ln (concn) versus time, giving a barrier Δ*G*[‡] for the formation of the C–C bond of 32.03(3) kcal/mol. This energy barrier has a correlation with both the C–C bond strength of the target C–C bond and the metal–carbon (M–C) bond strengths in the Pt^{II} complex.

It has been pointed out that C–C bond activation can be facilitated by lowering the energy of the C–C bond-cleaved oxidative addition products.²³ Metal–aryl complexes with electron-withdrawing substituents on the aryl group are generally more stable than those with electron-donating substituents.¹ Therefore, alkynes with electron-deficient aryl groups should produce more stable Pt^{II} complexes following C–C bond activation than alkynes with electron-rich aryl groups. Electron-withdrawing groups might also be expected to stabilize the Pt⁰-

(alkyne) complex but probably to a lesser extent.²⁴ By this approach, it might be possible to tune the C–C bond activation energy such that it would be thermodynamically favorable. The electron-rich alkyne bis(3,5-dimethylphenyl)acetylene was synthesized by a modified Sonogashira coupling method. The η²-coordinated Pt⁰ complex **3** was synthesized via eq 1 in high yield. Compound **3** displays a single ³¹P resonance at δ 94.14 (¹J_{P–Pt} = 2513.1 Hz) and has been characterized by X-ray analysis (Table 1).

Complex **3** was heated at 200 °C for 3 days, during which the reaction was monitored by ³¹P NMR spectroscopy. Similar to **1**, C–C bond activation was not observed under thermal conditions. Compound **3** was then irradiated in C₆D₆ for 6 h (λ > 300 nm), under which conditions C–C bond cleavage occurred cleanly. A high yield (90%) of the oxidative addition complex (dtbpe)Pt(3,5-dimethylphenyl)(3,5-dimethylphenylacetylide) **4** was obtained. The ³¹P NMR spectrum shows two singlets with platinum satellites, and the single-crystal X-ray structure shows the anticipated square-planar structure with the platinum-bound aryl group rotated 79.8° to the Pt square plane.

Quantitative reversion from **4** to **3** was observed by ³¹P NMR spectroscopy upon heating **4** at 80 °C. Therefore, this more electron-rich system also shows thermodynamically uphill behavior toward C–C cleavage. The first-order kinetics of the reverse reaction showed a barrier for the reverse reaction of 31.33(21) kcal/mol. Compound **4** is therefore slightly more labile toward reductive coupling than **2**.

Since the electron-rich substituents destabilized the oxidative addition complex, electron-withdrawing substituents should stabilize the C–C cleavage product. For this reason, the electron-deficient substrate bis(*p*-fluorophenyl)acetylene was attached to Pt to give (dtbpe)Pt(η²-bis(*p*-fluorophenyl)acetylene) **5** (³¹P NMR: δ 94.14, s, ¹J_{P–Pt} = 2510.7 Hz).

Analogous to the previous sets of Pt⁰ and Pt^{II} complexes, the C–C bond-activated complex was not observed upon heating **5**, yet photolysis produced the corresponding Pt^{II} complex (dtbpe)Pt(C₆H₄F)(C≡CC₆H₄F) **6**. The ³¹P NMR spectrum shows

- (17) Otsuka, S.; Nakamura, A. *Adv. Organomet. Chem.* **1976**, *14*, 245–283 and references therein.
 (18) Boag, N. M.; Green, M.; Grove, D. M.; Howard, J. A. K.; Spencer, J. L.; Stone, F. G. A. *J. Chem. Soc., Dalton Trans.* **1980**, 2170–2181.
 (19) (a) Bartik, T.; Happ, B.; Iglewsky, M.; Bandmann, H.; Boese, R.; Heimbach, P.; Hoffmann, T.; Wenschuh, E. *Organometallics* **1992**, *11*, 1235–1241. (b) Rosenthal, U.; Schulz, W. *J. Organomet. Chem.* **1987**, *321*, 103–117. (c) Tatsumi, K.; Hoffmann, R.; Templeton, J. L. *Inorg. Chem.* **1982**, *21*, 466–468. (d) Hey, E.; Weller, F.; Dehnicke, K. *Z. Anorg. Allg. Chem.* **1984**, *514*, 18–24. (e) Dewar, M. J. S.; Ford, G. P. *J. Am. Chem. Soc.* **1979**, *101*, 783–791. (f) Hartley, F. R. *Angew. Chem.* **1972**, *84*, 657–667. (g) Nelson, J. H.; Wheelock, K. S.; Cusachs, L. C.; Jonassen, H. B. *J. Am. Chem. Soc.* **1969**, *91*, 7005–7008. (h) Greaves, E. O.; Lock, C. J. L.; Maitlis, P. M. *Can. J. Chem.* **1968**, *46*, 3879–3891. (i) Dewar, M. J. S. *Bull. Soc. Chim. Fr.* **1951**, *18*, C79. (j) Chatt, J.; Duncanson, L. A. *J. Chem. Soc.* **1953**, 2939–2947.
 (20) Mavris, A.; Moustakali-Mavridis, I. *Acta Crystallogr.* **1977**, *B33*, 3612. The C≡C bond length in free diphenylacetylene is 1.198(4) Å.
 (21) Long, N. J.; Wong, C. K.; White, A. J. P. *Organometallics* **2006**, *25*, 2525–2532.
 (22) Iverson, C. N.; Lachicotte, R. J.; Muller, C.; Jones, W. D. *Organometallics* **2002**, *21*, 5320–5333.
 (23) Jun, C. H. *Chem. Soc. Rev.* **2004**, *33*, 610–618.

- (24) (a) Oshiki, T.; Yamada, A.; Kawai, K.; Arimitsu, H.; Takai, K. *Organometallics* **2007**, *26*, 173–182. (b) Yu, Y.; Smith, J. M.; Flaschenriem, C. J.; Holland, P. L. *Inorg. Chem.* **2006**, *45*, 5742–5751.

Table 2. Selected Bond Lengths and Angles for **2**, **4**, **6**, **8**, and **11**

| | 2 | 4 | 6 | 8 | 11 |
|-------------------|------------|------------|-----------|------------|------------|
| Bond Lengths (Å) | | | | | |
| Pt(1)–P(1) | 2.3168(5) | 2.3110(18) | 2.322(2) | 2.3220(4) | 2.3161(14) |
| Pt(1)–P(2) | 2.3253(5) | 2.3326(18) | 2.324(2) | 2.3070(4) | 2.3222(15) |
| Pt(1)–C(9) | 2.0943(18) | 2.098(7) | 2.088(8) | 2.0745(14) | 2.080(6) |
| Pt(1)–C(1) | 2.0001(18) | 2.017(7) | 1.982(9) | 1.9946(15) | 1.986(6) |
| C(1)–C(2) | 1.209(3) | 1.190(10) | 1.219(11) | 1.207(2) | 1.204(8) |
| C(2)–C(3) | 1.435(3) | 1.447(10) | 1.425(11) | 1.426(2) | 1.429(8) |
| Bond Angles (deg) | | | | | |
| C(9)–Pt(1)–C(1) | 80.32(7) | 84.9(3) | 81.4(3) | 82.37(6) | 82.5(2) |
| C(1)–Pt(1)–P(2) | 92.62(5) | 90.50(19) | 92.8(2) | 92.82(4) | 93.58(18) |
| P(2)–Pt(1)–P(1) | 87.731(16) | 87.90(7) | 87.98(7) | 88.413(13) | 87.95(5) |
| P(1)–Pt(1)–C(9) | 99.20(5) | 97.0(2) | 97.8(2) | 98.28(4) | 96.44(15) |
| Pt(1)–C(1)–C(2) | 171.16(16) | 173.5(7) | 170.0(7) | 168.76(13) | 170.2(6) |
| C(1)–C(2)–C(3) | 175.4(2) | 174.0(7) | 177.3(9) | 175.19(16) | 177.5(7) |

Table 3. Effect of Modification of Substrate on the Reductive Coupling Reaction

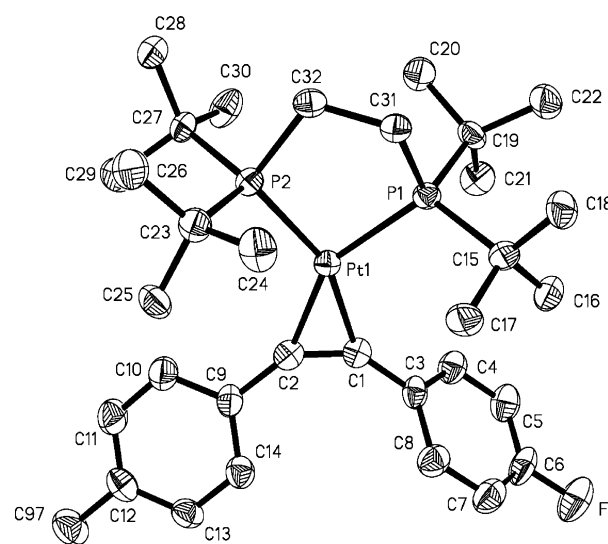
| substrate | reaction | ΔG^\ddagger (kcal/mol) | T (°C) |
|--|----------------------------------|--------------------------------|----------|
| bis(3,5-dimethylphenyl)acetylene | 4 \rightarrow 3 | 31.33 (3) | 80 |
| diphenylacetylene | 2 \rightarrow 1 | 32.03 (21) | 80 |
| bis(<i>p</i> -fluorophenyl)acetylene | 6 \rightarrow 5 | 32.78 (1) | 120 |
| bis(perfluorophenyl)acetylene | 8 \rightarrow 7 | 47.30 | 300 |
| <i>p</i> -tolyl- <i>p</i> -fluorophenylacetylene | 10 \rightarrow 9 | 33.32 (17) | 100 |
| | 11 \rightarrow 9 | 32.10 (2) | 100 |

two singlets at δ 71.35 ($^1J_{P-Pt} = 1963.4$ Hz, P trans to acetylide) and 77.74 ($^1J_{P-Pt} = 1296.6$ Hz, P trans to *p*-fluorophenyl).

Complex **6** showed similar behavior to the previous two Pt^{II} complexes, quantitatively reverting to **5** upon heating at 120 °C. This electron-deficient system also shows thermodynamically uphill behavior toward C–C cleavage. The first-order kinetics of the reverse reaction showed a barrier for the reverse reaction of 32.78(1) kcal/mol, indicating that **6** is slightly more stable toward reductive coupling than **2** (~ 3 times slower).

As an electron-deficient substrate stabilizes the corresponding Pt^{II} complex, a more electron-deficient substrate might permit thermal C–C cleavage. The η^2 -coordinated Pt⁰ complex (dtbpe)-Pt(η^2 -bis(pentafluorophenyl)acetylene) (**7**) was synthesized and fully characterized (^{31}P NMR: δ 94.26, s, $^1J_{P-Pt} = 2636.9$ Hz). A light yellow solution of **7** in C_6D_6 was heated at 300 °C for 3 days in a sealed tube. The reaction was monitored by ^{31}P NMR spectroscopy periodically but no C–C activated product was observed. During this high-temperature reaction of **7**, no decomposition was seen and the color of the solution remained light yellow. Upon overnight photolysis of **7**, the C–C bond cleavage product (dtbpe)Pt(C_6F_5)($\text{C}\equiv\text{CC}_6\text{F}_5$) (**8**) was obtained. The ^{31}P NMR spectrum shows two singlets at δ 77.0 ($^1J_{P-Pt} = 2442.77$ Hz) and 79.6 ($^1J_{P-Pt} = 2273.1$ Hz).

In order to measure the effect of the electron-withdrawing groups on the C–C and M–C bond strengths, complex **8** was heated at 300 °C and reversion to **7** was monitored by ^{31}P NMR spectroscopy. From the observed rate, the energy barrier for the reversion of **8** to **7** was estimated to be 47.30 kcal/mol. The tremendous thermal stability of **8** can be attributed to the high strength of the Pt–aryl bond due to the presence of two ortho-fluorines. The enhancement of metal–aryl bond strength with the number of ortho-fluorines has been impressively demonstrated in the literature.²⁵ This demonstrates that while electron-

**Figure 4.** Molecular structure of **9** (ORTEP diagram, 30% probability ellipsoids). Final R indices [$I > 2\sigma(I)$], $R1 = 0.0472$. Monoclinic, $P2_1/c$.

withdrawing group substitution has substantially stabilized the Pt^{II} complex, this stabilization was not enough to render the forward C–C cleavage reaction thermodynamically downhill.

Variations in the stability of the complexes upon modification of the substrate by adding electron-donating and electron-withdrawing groups are summarized in Table 3. Electron-withdrawing groups have a profound effect upon stabilizing the Pt^{II} C–C cleavage product. Electron-donating groups, in comparison, have only a small effect. It is noteworthy that earlier methyl hydride reductive elimination studies on platinum showed that electron-withdrawing groups on the phosphine led to more rapid elimination whereas electron-donating groups slowed elimination,²⁶ as in this case stabilization of the platinum product by the phosphine dominates the rate of elimination.

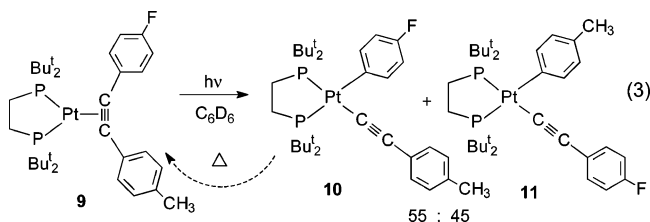
The data in Table 3 indicate that electron-deficient substituents on the acetylene provide the more stable C–C bond-activated complexes while electron-rich substituents destabilize the Pt^{II} complexes. Therefore, use of a heterosubstituted substrate like *p*-tolyl-*p*-fluorophenylacetylene might be expected to show selective C–C bond activation. The heterosubstituted alkyne *p*-tolyl-*p*-fluorophenylacetylene was synthesized and reacted with $\text{Pt}(\text{COD})_2$ as shown in eq 1. The η^2 -coordinated Pt⁰ complex of (dtbpe)Pt(η^2 -*p*-tolyl-*p*-fluorophenylacetylene) was

(25) Clot, E.; Besora, M.; Mégret, C.; Eisenstein, O.; Oelckers, B.; Perutz, R. *N. Chem. Commun.* **2003**, 490–491.

(26) Abis, L.; Sen, A.; Halpern, J. *J. Am. Chem. Soc.* **1978**, *100*, 2915–2916.

fully characterized (Figure 4), and the ^{31}P NMR spectrum of this Pt^0 derivative shows a singlet at δ 94.25 ($^1J_{\text{P-Pt}} = 2506.9$ Hz), despite the fact that the two phosphorus nuclei are opposite different aryl groups.

Since the Pt–aryl bond with the electron-deficient aryl is expected to be stronger than the Pt–aryl bond with the electron-rich aryl, C–C bond cleavage was expected to form a Pt–aryl bond with the electron-withdrawing group-substituted aryl. Before irradiation with UV light, complex **9** was heated at 200 °C for a day and the corresponding C–C activated Pt^{II} complex was not observed. Irradiation of complex **9** with UV light overnight led to 96% conversion to a mixture of the Pt^{II} complexes (dtbpe)Pt(*p*-fluorophenyl)(*p*-tolylacetylide) **10** and (dtbpe)Pt(*p*-tolyl)(*p*-fluorophenylacetylide) **11**, observed in a 55:45 ratio, respectively, by ^{31}P NMR spectroscopy (eq 3). There were four phosphorus resonances observed at δ 70.9 ($^1J_{\text{Pt-P}} = 2007.3$ Hz, major), 71.2 ($^1J_{\text{Pt-P}} = 1980.0$ Hz, minor), 77.7 ($^1J_{\text{Pt-P}} = 1298.3$ Hz, major), and 77.8 ($^1J_{\text{Pt-P}} = 1259.1$ Hz, minor), two for each complex. The spectral assignments were made based upon analogies to symmetric activation products **6** and **2**. The phosphorus resonance in complex **6** for the P trans to *p*-fluorophenyl showed a coupling constant of $^1J_{\text{Pt-P}} = 1296.6$ Hz, which is very similar to the value observed for the phosphorus resonance at δ 77.7. Therefore, the major product resonance at δ 77.7 can be assigned to the P trans to *p*-fluorophenyl in **10**. The other major resonance at δ 70.9 is assigned to the P trans to *p*-tolylacetylide in **10**. Hence the phosphorus resonance at δ 77.8 ($^1J_{\text{Pt-P}} = 1259.1$ Hz) can be assigned to the P trans to *p*-tolyl in **11**, and the one at δ 71.2 ($^1J_{\text{Pt-P}} = 1980.0$ Hz) to the P trans to acetylide in **11**.



The mixture of the complexes **10** and **11** was recrystallized and a single-crystal structure determination showed one of the two possible products, **11** (Figure 5). There was no evidence for disorder of the methyl and fluoro groups, as the bond distances were noticeably different (C–F = 1.3 Å and C–Me = 1.5 Å).

Similar to the previous Pt^{II} oxidative addition complexes, the mixture of **10** and **11** showed reversion to Pt^0 complex **9** upon heating at 100 °C. However, the rates of reversion from **10** and **11** to **9** were slightly different for the two compounds. The kinetics of the reversion reactions of **10** → **9** and **11** → **9** were monitored and the rate constants were determined from the slopes of the first-order plots (Figure 6), giving $\Delta G^\ddagger = 33.32$ –(17) kcal/mol for **10** and 32.10(2) kcal/mol for **11**.

An analysis of the kinetic selectivity in the photolysis of **9** allows a comparison of the energies of the C–C cleavage products to be made. Since photolysis of **9** gave almost a 1:1 ratio of products **10** and **11**, this implies similar barriers to C–C cleavage. This reaction is photochemical, and the transition states need not lie at the same energies as in the thermal pathways, since excited states are involved. However, if we assume that the energetics of the excited-state pathways follow those of the

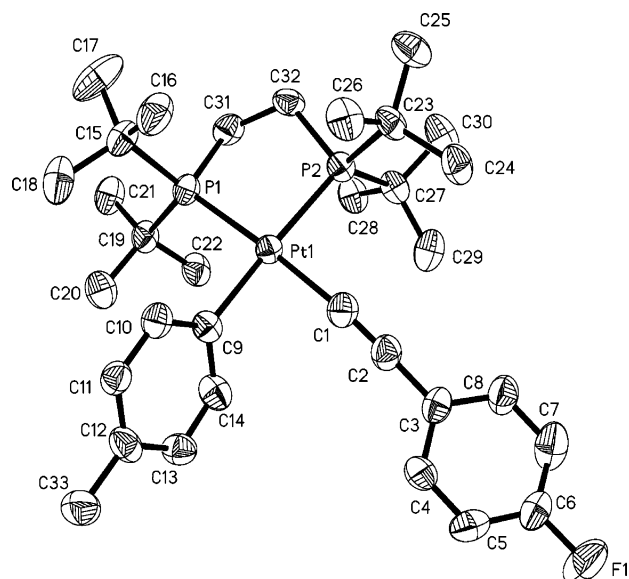


Figure 5. Molecular structure of (dtbpe)Pt(*p*-tolyl)(C≡CC₆H₄F) **11** (ORTEP diagram, 30% probability ellipsoids).

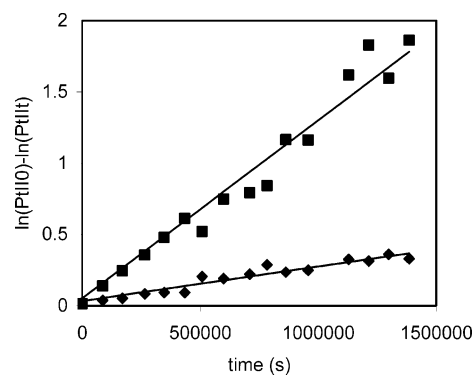


Figure 6. Reverse reactions **10** → **9** (◆) and **11** → **9** (■) at 100 °C in C₆H₆.

thermal pathways, then the energies of the transition states leading to the two products **10** and **11** should be similar ($\Delta\Delta G^\ddagger \approx 0.1$ kcal/mol). On the other hand, reductive coupling barriers differ by 1.22 kcal/mol, suggesting a thermodynamic preference for the more electron-deficient aryl group being attached to Pt (Hammond postulate). Therefore, the enhanced stability observed for C–C cleavage products containing electron-deficient aryl groups can be associated with a stabilization of the Pt^{II} product rather than changing the energy of the transition state for C–C cleavage.

With regard to kinetic selectivity, since the C–C bond-activated product **10** was 55% while the C–C bond-activated product **11** was 45%, greater selectivity in C–C bond activation might be achieved by increasing the difference between electron deficiency and richness on the two target aryl groups.

Conclusions

Pt^0 complexes of η^2 -coordinated diarylacetylenes have been synthesized and fully characterized along with the corresponding C–C bond-activated Pt^{II} complexes. C–C bond activation occurred only under photochemical conditions. Under thermal conditions, up to 300 °C, C–C bond activation was not observed. However, reductive coupling, that is, $\text{Pt}^{\text{II}} \rightarrow \text{Pt}^0$, did occur under thermal conditions and allowed determination of

the barrier to C–C bond formation. According to the activation energy barriers for the reverse reaction, electron-deficient substituents stabilize the Pt^{II} complex while electron-rich ones destabilize it. The transition state is not affected as much, leading to the notion that the energy barrier for C–C bond formation can be tuned by modifying the substrate by adding the EDGs and EWGs. In no case was sufficient stabilization obtained to change the overall energy profile and make the activation reaction thermodynamically downhill.

The C–C cleavage reaction in a substrate containing both electron-donating and electron-withdrawing substituents has produced 55% activation product through the C–C bond adjacent to the EWG-substituted aryl ring and 45% activation product through the one adjacent to the EDG-substituted aryl, implying that modest kinetic selectivity can be obtained in C–C bond cleavage. In this report, all the activated C–C bonds were sp–sp²-type hybridized carbons. Further studies will be required with similar Pt⁰– η^2 -acetylene complexes to extend these cleavage results to sp–sp³-hybridized C–C bonds.

Experimental Section

General Considerations. All experiments were carried out under a nitrogen atmosphere, either on a high-vacuum line using modified Schlenk techniques or in a Vacuum Atmosphere Corp. glove box unless otherwise stated. The solvents were available commercially and were distilled from dark purple solutions of benzophenone ketyl.

¹H, ¹³C{¹H}, and ³¹P{¹H} NMR spectra were recorded on Bruker Avance-400, Bruker AMX-400, and Bruker Avance-500 spectrometers. All ¹H chemical shifts were referenced to residual proton resonances or to tetramethylsilane (TMS) in the deuterated solvents. An external standard of 85% H₃PO₄ was used to reference the ³¹P{¹H} NMR data. All crystal structures were determined by use of a Siemens-SMART 3-Circle CCD diffractometer. All photolysis experiments were performed with an Oriel arc source using a 200 W Hg(Xe) lamp in sealed NMR tubes. Elemental analyses were obtained from Desert Analytics. Diphenylacetylene was obtained from commercial sources and Pt(COD)₂,^{27,28} bis(pentafluorophenyl)acetylene,² and bis(di-*t*-butylphosphino)ethane³⁰ were synthesized according to reported procedures. Kinetic analyses were carried out by use of Microsoft Excel with the Solver statistics module added.³¹ Errors are reported as standard deviations. Due to the slowness of the reductive coupling reactions, data from <3 half-lives was used in the kinetic determinations of **2**, **4**, and **10**. Reductive coupling in **8** was so slow that the rate was estimated from a single point (10% change after 3.5 h at 300 °C).

Preparation of (dtbpe)Pt(η^2 -PhC≡CPh) (1). Diphenylacetylene (8.66 mg, 48.6 μ mol) was dissolved in 0.7 mL of C₆D₆ and added to white-beige crystals of Pt(COD)₂ (20 mg, 48.6 μ mol). As the color of the solution changed from colorless to light yellow, a solution of dtbpe (15.47 mg, 48.65 μ mol) in 0.3 mL of C₆D₆ was added. The above order and time of adding the dtbpe is crucial to obtaining good yields of **1**. The resultant solution was transferred into a sealed NMR tube and then heated at 80 °C for 40 min, allowing all of the dtbpe to coordinate to Pt. The reaction was monitored by ³¹P{¹H} NMR spectroscopy, and once all of the free dtbpe was consumed and **1** was produced, solvent and free COD [released from the initial Pt(COD)₂ precursor] were removed under high vacuum. The light yellow powder **1** was taken back into the glove box and redissolved in C₆H₆. It was

crystallized at room temperature via solvent evaporation. Yield: 27.6 mg (82%) of colorless air-sensitive crystals of **1**. ¹H NMR (C₆D₆) δ 7.752 (d, ³J_{H–H} = 7.5 Hz, 4H, *o*-C₆H₅), 7.244 (t, 4H, *m*-C₆H₅), 6.984 (t, ³J_{H–H} = 7.5 Hz, 2H, *p*-C₆H₅), 1.351 (d, ²J_{H–P} = 6.5 Hz, 4H, P-CH₂), 1.144 [virtual t, ³J_{H–P} = 12.5 Hz, 36H, C-(CH₃)₃]. ¹³C{¹H} NMR (CDCl₃) δ 26.61 (d, P-CH₂), 30.95 (m, C-CH₃), 35.46 (t, ¹J_{C–P} = 31.91 Hz, P-C-), 125.27 (s, *ipso*-C), 128.74 (s, *p*-C), 129.18 (s, *m*-C), 132.45 (s, *o*-C), 141.57 (m, C≡C). ³¹P NMR (C₆D₆) δ 94.23 (s, with platinum satellites, ¹J_{Pt–P} = 2516.4 Hz). Anal. Calcd for C₃₂H₅₀P₂Pt: C, 55.54; H, 7.29. Found: C, 55.39; H, 7.25.

Preparation of (dtbpe)Pt(-Ph)(-C≡CPh) (2). Ten milligrams of **1** was dissolved in 1 mL of C₆D₆ and placed into an NMR tube with a Teflon stopcock. The sample was irradiated with UV light (λ > 300 nm) for 4 h. The sample was crystallized by solvent evaporation at room temperature. Colorless and air-stable crystals of **2** (8.9 mg, 89%) were obtained. ¹H NMR (C₆D₆) δ 1.03 [d, ³J_{H–P} = 10.4 Hz, 18H, C-(CH₃)₃], 1.34 [d, ³J_{H–P} = 10.4 Hz, 18H, C-(CH₃)₃], 1.12–1.22 (m, 4H, -CH₂), 6.97 (t, 3H, *m*-H and *p*-H), 7.29 (distorted t, 3H, *m*-H and *p*-H), 7.42 (d, 2H, *o*-H), 7.97 (t, 2H, *o*-H). ¹³C{¹H} NMR (C₆D₆) δ 24.1 (m, P-CH₂), 26.58 (m, P-CH₂), 30.71 [m, -(CH₃)₃], 36.2 (d, ¹J_{C–P} = 56.4 Hz, P-CH₂), 36.78 (d, ¹J_{C–P} = 65.2 Hz, P-CH₂), 111.33 (d, ³J_{C–P} = 120 Hz, C≡C-Ph), 112.9 (d, ³J_{C–P} = 680 Hz, C≡C-Ph), 122.53, 125.14, 127.62, 131.72, 140.51 (aromatic carbon resonances). ³¹P NMR (C₆D₆) δ 71.36 (s, with Pt satellites, ¹J_{Pt–P} = 1978.3 Hz, 1P, P trans to acetylide), 77.45 (s, with Pt satellites, ¹J_{Pt–P} = 1250.6 Hz, 1P, P trans to -Ph). Anal. Calcd for C₃₂H₅₀P₂Pt: C, 55.54; H, 7.29. Found: C, 55.18; H, 7.00.

Preparation of (dtbpe)Pt(η^2 -RC≡CR), R = 3,5-xylyl (3), p-C₆H₄F (5), or C₆F₅ (7). These compounds were prepared by procedures analogous to that described above for **1**. Full details including ¹H, ³¹P, and ¹³C NMR data, analyses, and X-ray structures are given in the Supporting Information.

Preparation of (dtbpe)Pt(R)(C≡CR), R = 3,5-xylyl (4), p-C₆H₄F (6), or C₆F₅ (8). These compounds were prepared by photochemical procedures analogous to that described above for **2**. Full details including ¹H, ³¹P, and ¹³C NMR data, analyses, and X-ray structures are given in the Supporting Information.

Synthesis of p-Tolyl-p-fluorophenylacetylene. Cuprous iodide (0.25 g, 1.25 mmol) was added to a triethylamine solution (50 mL) of *t*-Cl₂-Pd(PPh₃)₂ (0.90 g, 1.25 mmol), iodo-*p*-fluorobenzene (4 g, 18 mmol), and *p*-tolylacetylene (20.8 g, 18 mmol) in a round-bottom flask equipped with a stir bar and a condenser under a nitrogen atmosphere. The mixture was refluxed for 6 h and then water was added. The organic layer was extracted with ether and the extract was dried over anhydrous Na₂SO₄. The solution was filtered and the ether was removed under reduced pressure until product started to precipitate. The residue was left for crystallization in ether at –10 °C. White crystals of *p*-tolyl-*p*-fluorophenylacetylene (2.61 g) were obtained in 69.0% yield. ¹H NMR (CDCl₃) δ 2.39 (s, CH₃), 7.05 (t, *J* = 17.4 Hz), 7.18 (d, *J* = 7.9 Hz), 7.44 (d, *J* = 8.0 Hz), 7.52 (m). ¹³C{¹H} NMR (CDCl₃) δ 21.5 (s, CH₃), 87.6 (s, C≡C), 89.0 (s, C≡C), 115.0 (d, ²J_{C–F} = 22.9 Hz, *m*-C), 119.0 (s), 119.9 (s), 129.0 (s), 131.3 (s), 133.3 (d, ³J_{C–F} = 7.0 Hz, *o*-C on fluorophenyl), 138.2 (s), 162.6 (d, ¹J_{C–F} = 251.5 Hz, C–F). ¹⁹F NMR (CDCl₃) δ 2.9 (s, *p*-F) (referenced to fluorobenzene).

Preparation of (dtbpe)Pt(η^2 -*p*-Fluorophenyl-*p*-tolylacetylene) (9). White crystals of *p*-fluorophenyl-*p*-tolylacetylene (30.65 mg, 0.146 mmol) were dissolved in 4 mL of C₆D₆. In another vial, white crystals of dtbpe (46.41 mg, 0.146 mmol) were dissolved in 2 mL of C₆D₆. White-beige powder of Pt(COD)₂ (60 mg, 0.146 mmol) was placed in a separate vial. First, the colorless solution of *p*-fluorophenyl-*p*-tolylacetylene was transferred onto the Pt(COD)₂ and stirred for 10 s. While the color of the solution was turning from colorless to orange, the solution of dtbpe was transferred in. The resultant light yellow solution was stirred for 3 min. The solution was transferred into a sealed tube and heated at 80 °C for 1.5 h. One milliliter of the solution was taken for an NMR experiment. According to the ³¹P NMR spectrum,

(27) McDermott, J. X.; White, J. F.; Whitesides, G. M. *J. Am. Chem. Soc.* **1976**, *98*, 6521–6528.

(28) Osborn, T. A.; Wilkinson, G.; Mrowca, J. *J. Inorg. Synth.* **1990**, *28*, 77.

(29) Gastinger, R. G.; Tokas, E. F.; Rausch, M. D. *J. Org. Chem.* **1978**, *43*, 159–161.

(30) Porschke, K. R.; Pluta, C.; Proft, B.; Lutz, F.; Kruger, C. K. *Z. Naturforsch. B: Chem. Sci.* **1993**, *48*, 608–626.

(31) Billo, E. J. *Excel for Chemists, A Comprehensive Guide*; Wiley-VCH: New York, 1997; pp 297–299.

~4% of the Pt(COD)₂ was not reacted with *p*-fluorophenyl-*p*-tolylacetylene. To obtain only **9**, the solution was heated at 100 °C for 1 day. The sealed tube was attached to the vacuum line, and both solvent and COD were removed. The light yellow powder **9** was taken back into the glovebox and redissolved in C₆H₆ for crystallization. Colorless and air-sensitive crystals of **9** (82.3 mg, 78%) were obtained after 3 days upon crystallization at room temperature via solvent evaporation: ¹H NMR (C₆D₆) δ 1.14 (t, ³J_{H-P} = 20 Hz, 36H, C-CH₃), 1.35 (d, ²J_{H-P} = 7 Hz, 4H, -CH₂), 2.16 (s, 3H, *p*-CH₃), 6.90 (t, 2H, *m*-H on Ph-CH₃), 7.05 (d, 2H, *m*-H on Ph-F), 7.60 (t, 4H, *o*-H). ¹³C{¹H} NMR (CDCl₃) δ 21.20 (s, 1 C, *p*-CH₃), 25.78 (m, 2 C, P-CH₂), 30.16 (s, 12 C, C-CH₃), 34.59 (m, 4 C, P-C), 114.35 (d, 2 C, *ipso*-C), 128.38 (s, *p*-C on Ph-CH₃), 129.21 (s, 4 C, *m*-C), 133.97 (s, 4 C, *o*-C), 162 (s, 2 C, C≡C), 170 (d, J_{C-F} = 1800 Hz, *p*-C on Ph-F). ³¹P NMR (C₆D₆) δ 94.25 (s, with platinum satellites, ¹J_{Pt-P} = 2506.9 Hz). Anal. Calcd for C₃₃H₅₁FP₂Pt: C, 54.74; H, 7.11. Found: C, 54.93; H, 6.84.

Preparation of both (dtbpe)Pt(*p*-Fluorophenyl)(*p*-tolylacetylide) (10**) and (dtbpe)Pt(*p*-tolyl)(*p*-Fluorophenylacetylide) (**11**).** Twenty milligrams of **9** was dissolved in 1 mL of C₆D₆, and the light yellow solution was placed in a sealed NMR tube. The sample was irradiated overnight, and 96% conversion to **10** and **11** was observed via ³¹P NMR spectroscopy. No further conversion or formation of Pt^{II} complex was observed after irradiation for one more day. The NMR tube was taken back into the glove box and the solution was transferred to a vial. It was left for crystallization at room temperature by solvent evaporation. After 4 days, colorless and air-stable crystals of **10** and **11** (14.2 mg, 71%) were obtained. ¹H NMR (CDCl₃) δ 1.13 (d of m, 36H, C-(CH₃)₃ trans to *p*-fluorophenyl and trans to *p*-tolyl), 1.37 (d of m, 36H, C-(CH₃)₃ trans to *p*-fluorophenylacetylide and trans to *p*-tolylacetylide), 2.07 (s, 6H, *p*-methyl in *p*-tolyl and *p*-tolylacetylide), 6.7–6.94 (m, 12H, *m*-H in *p*-fluorophenyl and *p*-tolyl and *o*-H and *m*-H in *p*-fluorophenylacetylide and *p*-tolylacetylide), 7.33 (m, 2H, *o*-H in *p*-tolyl), 7.41 (m,

2H, *o*-H in *p*-fluorophenyl). ¹³C{¹H} NMR (CDCl₃) δ 21–24 (4 m, P-CH₂ cis and trans to Pt-Ph in both complexes), 26.6 (s, *p*-CH₃ both in *p*-tolyl and *p*-tolylacetylide), 30.2 [m, C-(CH₃)₃ cis and trans to Pt-Ph in both complexes], 36.2 (d of m, P-C cis and trans to Pt-Ph in both complexes), 113.2 and 115.8 (dd, Pt-C≡C in both complexes), 114.4 (d, Pt-C≡C in both complexes), 127–134 (six resonances, aromatic carbons in both complexes), 139 (m, *o*-C in *p*-tolylacetylide and *p*-fluorophenylacetylide in both complexes), 160.5 (d, *p*-C-F in both *p*-fluorophenyl and *p*-fluorophenylacetylide). ³¹P NMR (CDCl₃) δ 70.9 (s, with platinum satellites, ¹J_{Pt-P} = 2007.3 Hz, 1P, P trans to *p*-tolylacetylide), 71.2 (s, with platinum satellites, ¹J_{Pt-P} = 1980.0 Hz, 1P, P trans to *p*-fluorophenylacetylide), 77.7 (s, with platinum satellites, ¹J_{Pt-P} = 1298.3 Hz, P trans to *p*-fluorophenyl), 77.8 (s, with platinum satellites, ¹J_{Pt-P} = 1259.1 Hz, P trans to *p*-tolyl). Anal. Calcd for C₃₃H₅₁FP₂Pt·C₆H₆: C, 58.39; H, 7.17. Found: C, 59.14; H, 7.42.

Acknowledgment. Acknowledgement is made to the U.S. Department of Energy for support (Grant FG02-86ER13569), to William Brennessel for his help in reorganizing the single-crystal structure analysis reports, and to Professor Richard Eisenberg for his suggestions about Pt complexes and photolysis reactions.

Supporting Information Available: Details of preparations of **3**, **5**, **7**, **4**, **6**, **8**, and alkynes; data collection parameters; crystal data for complexes **1–9** and **11**; UV–vis spectra for complexes **1**, **3**, and **7**; and kinetics for reactions **2** → **1**, **4** → **3**, and **6** → **5**. This material is available free of charge via the Internet at <http://pubs.acs.org>.

JA071698K